



## Comparative profiling and exposure assessment of microplastics in differently sized Manila clams from South Korea by $\mu$ FTIR and Nile Red staining

Maria Krishna de Guzman<sup>a,b</sup>, Mirjana Andjelković<sup>c</sup>, Vesna Jovanović<sup>d</sup>, Jaehak Jung<sup>e</sup>, Juyang Kim<sup>e</sup>, Lea Ann Dailey<sup>f</sup>, Andreja Rajković<sup>b</sup>, Bruno De Meulenaer<sup>b</sup>, Tanja Ćirković Veličković<sup>a,b,d,g,\*</sup>

<sup>a</sup> Center for Food Chemistry and Technology, Ghent University Global Campus, Incheon, South Korea

<sup>b</sup> Department of Food Technology, Safety, and Health, Faculty of Bioscience Engineering, Ghent University, Ghent, Belgium

<sup>c</sup> Sciensano, Brussels, Belgium

<sup>d</sup> Faculty of Chemistry, Centre of Excellence for Molecular Food Sciences, University of Belgrade, Belgrade, Serbia

<sup>e</sup> Korea Institute of Analytical Science and Technology, Seoul, South Korea

<sup>f</sup> Department of Pharmaceutical Sciences, University of Vienna, Vienna, Austria

<sup>g</sup> Serbian Academy of Sciences and Arts, Belgrade, Serbia

### ARTICLE INFO

#### Keywords:

Manila clam  
Nile red  
 $\mu$ FTIR  
Fluorescence microscopy  
Microplastics  
Exposure

### ABSTRACT

The accumulation of microplastics in marine organisms is an emerging concern. Due to trophic transfer, the safety of seafood is under investigation in view of the potential negative effects of microplastics on human health. In this study, market samples of Manila clams (*Ruditapes philippinarum*) from South Korea were segregated into two groups of considerably different size ( $p < 0.05$ ), namely small clams with shell length of  $40.69 \pm 3.97$  mm, and large clams of shell length  $51.19 \pm 2.86$  mm. Comparative profiling of the number, size, shape, and polymer type of microplastics were performed using  $\mu$ FTIR imaging and Nile red staining. Overall,  $\mu$ FTIR detected only 1559 microplastics while 1996 microplastics were counted based on staining from 61 Manila clams (30 small and 31 large), leading to an overestimation of 18 to 75 %. Comparable microplastics concentration, based on  $\mu$ FTIR, were observed at  $2.70 \pm 1.66$  MP/g or  $15.64 \pm 9.25$  MP/individual for the small samples, and  $3.65 \pm 1.59$  MP/g or  $41.63 \pm 16.90$  MP/individual for the large ones ( $p > 0.05$ ). Particle diameters of 20–100  $\mu$ m was the most dominant, accounting for 44.6 % and 46.5 % of all microplastics from the small and large groups, respectively. Particles, with a circularity (resemblance to a circle) value between 0.6 and 1.0, were the most prevalent, followed by fragments and fibers. At least 50 % of microplastics from the small and large samples were polystyrene, making it the most abundant polymer type. Despite the substantial difference in the size of the animals, only a weak to moderate correlation was observed between microplastics content and the physical attributes of the clams such as shell length and weight, (soft) tissue weight, and total weight (Spearman's coefficient  $< 0.5$ ). The estimated intake of microplastics by the Korean population was 1232 MP/person/year via small clams, 1663 MP/person/year via large clams, and 1489 MP/person/year via clams independent of size.

### 1. Introduction

Since the term 'microplastics' (MP) surfaced in 2004 (Thompson et al., 2004), its presence in the environment and food chain has become an area of great interest and concern. Contamination of air, land, aquatic bodies, and fauna by MP is being investigated. To date, MP are proven to

exist in marine biota (De Witte et al., 2014; Mathalon and Hill, 2014; Vandermeersch et al., 2015; Digka et al., 2018b; Khoironi et al., 2018; Phuong et al., 2018; Renzi et al., 2018), birds (Cadée, 2002; Mallory, 2008), indoor air (Dris et al., 2016), food such as drinking water, honey, sugar, tea, and alcohol (Yang et al., 2015; Cox et al., 2019), and in the different zones of the ocean (Ng and Obbard, 2006; Browne et al., 2011;

**Abbreviations:** MP, microplastics; NR, Nile red; NRS, Nile red staining; SC, Small clams; LC, Large clams.

\* Corresponding author at: Center for Food Chemistry and Technology, Ghent University Global Campus, Incheon, South Korea.

E-mail addresses: [tanja.velickovic@ghent.ac.kr](mailto:tanja.velickovic@ghent.ac.kr), [tcirkov@chem.bg.ac.rs](mailto:tcirkov@chem.bg.ac.rs) (T. Ćirković Veličković).

<https://doi.org/10.1016/j.marpolbul.2022.113846>

Received 11 February 2022; Received in revised form 9 June 2022; Accepted 10 June 2022

Available online 25 June 2022

0025-326X/© 2022 The Authors. Published by Elsevier Ltd. This is an open access article under the CC BY-NC-ND license (<http://creativecommons.org/licenses/by-nc-nd/4.0/>).

Van Cauwenberghe et al., 2013; Eriksen et al., 2014; Yang et al., 2015) and freshwater which includes the surface, water column, and bottom sediment (Li et al., 2018). By definition, MP are plastics smaller than 5 mm (Arthur et al., 2009). They are derived from synthetic polymers that are either initially manufactured in microscopic sizes (primary MP), such as exfoliating agents in cosmetic products, or generated via the breakdown of large plastic fragments (secondary MP) due to chemical, physical, and biological processes (Cole et al., 2011; Van Cauwenberghe et al., 2015). Globally, 92.4 % of the plastics in the oceans are MP (Eriksen et al., 2014), making it the most prevalent form of marine plastic pollution.

Given the small size and pervasive nature of MP, ingestion by several marine species (mollusks, crustaceans, fish, and echinoderms) has been observed. Once ingested, MP are distributed and accumulate in various organs such as gills, gut, liver, kidneys (Lu et al., 2016; Deng et al., 2017; Plee and Pomory, 2020), and respiratory structures (Mohsen et al., 2021). This can result in unfavorable health effects that include decreased food intake and reduced growth rate (Besseling et al., 2013), lower fertility (Sussarellu et al., 2016), inflammation (Von Moos et al., 2012), oxidative stress (Lu et al., 2016), and higher immune response (Browne et al., 2008; Canesi et al., 2015; Green, 2016; Rist et al., 2016). Even though ingestion was not observed to be fatal, chronic effects are a critical matter. Increasingly, human exposure to MP and the possibility of associated health risks has become a growing concern. For the risk to be estimated accurately, information gaps on the extent of human exposure to MP must be filled. Specifically, data regarding the MP quantity, size, shape, and chemical composition for each relevant exposure route (e.g., ingestion, inhalation, dermal contact) must be gathered.

The transfer of MP through the food chain is one of the predominant exposure routes for humans. Among seafood products, the consumption of bivalves such as clams, oysters, and mussels, presents a high risk of transposal. Compared to fish and some type of shellfish, where the gut is removed during food preparation, most bivalves are commonly eaten with an intact digestive tract (Rainieri and Barranco, 2019). As shown in numerous studies, the digestive tract is where MP accumulate, especially in bivalves (Von Moos et al., 2012; Lu et al., 2016; González-Soto et al., 2019). Even though depuration was shown to decrease the plastic content in the stomach, >55 % still remained afterward (Van Cauwenberghe and Janssen, 2014). Hence, consuming such species will lead to higher MP exposure, especially in regions with a seafood-rich diet such as South Korea, with an annual intake of 58.4 kg of seafood per person (10.6 kg corresponds to bivalves) (Food and Agriculture Organization of the United Nations (FAO), 2016).

A standard protocol for MP quantification still does not exist. Two of the most commonly used techniques based on literature are Nile red staining (NRS) and  $\mu$ FTIR spectroscopy. Fluorescent tagging of MP using Nile red (NR) has gained widespread use because of its inexpensive nature and its affinity to a wide range of polymers (Prata et al., 2021). In addition, smaller MP particles ( $\geq 3 \mu\text{m}$ ) can be easily detected and visualized due to the high fluorescence intensity of the dye (Shruti et al., 2022). With the advancement in image processing technology, a few tools for automated measurement of number and size of stained MP are now available (Prata et al., 2019, 2020). Despite these advantages, NRS lacks the ability to identify polymer types, which  $\mu$ FTIR spectroscopy can provide. For focal plane array (FPA)  $\mu$ FTIR, a large area containing MP can even be scanned easily with simultaneous visualization and collection of spectra (Elert et al., 2017; Cabernard et al., 2018). However, this approach is still time-consuming and requires expensive equipment combined with a well-trained operator (Primpke et al., 2017). A further important limitation of  $\mu$ FTIR is the current detection limit of  $\sim 20 \mu\text{m}$ , meaning that MP in the low micron range, as well as nanoplastics, cannot be analyzed reliably (Cabernard et al., 2018).

Exposure of humans to MP originating from shellfish has been previously quantified using both  $\mu$ FTIR or  $\mu$ Raman spectroscopy (Cho et al., 2019, 2021). Because of the size limitation of both techniques,

underestimation is inevitable on account of proper chemical characterization of MP debris. Aside from this, current protocols describe that a manual inspection of the filter is required to pre-select suspected MP prior to chemical characterization, a process which is prone to errors and bias. In this respect, a combination of staining and  $\mu$ FTIR is needed to completely capture the wide range of MP sizes present in the samples.

In this study, we used both NRS and  $\mu$ FTIR spectroscopy to measure the MP quantity, morphology, size, and chemical nature, and investigate the effect/s of shell size and age on the accumulation of MP in Manila clams (*Ruditapes philippinarum*) in South Korea. The samples were segregated into two groups: small clams (SC) and large clams (LC) with shell length of  $40.69 \pm 3.97 \text{ mm}$  and  $51.19 \pm 2.86 \text{ mm}$ , respectively. Comparative profiling of SC and LC was performed using  $\mu$ FTIR- and NRS-based measurements to obtain a comprehensive set of information on the MP content and overcome the drawbacks associated with using one technique alone. In addition, a software-guided strategy for quantification and classification was employed to avoid the bias inherent to manual inspection. Lastly, exposure assessment was carried out to estimate the level of exposure of Korean consumers to MP through consumption of Manila clams.

## 2. Materials and methods

### 2.1. Reagents, materials, and equipment

All sample preparation, filtration, and glassware cleaning steps were performed inside a laminar flow cabinet (Daihan Scientific, SLCV1-12) to prevent contamination from indoor airborne MP. Deionized water, reagents, and solutions were filtered using  $0.22 \mu\text{m}$  PTFE membrane (Hyundai micro Co., Ltd., HP020025D) filters before use. The filtered water was used to wash all glassware prior to experiments. All samples were covered with aluminum foil when moved outside the laminar flow hood. Cotton laboratory coats were worn throughout the procedure (Cho et al., 2019). GF/A glass microfibre filters (Whatman, 1820-047),  $1.6 \mu\text{m}$ , were used for filtration of samples after digestion. KOH (Daejung, 6584-4400) was used for digestion of organic matter while  $\text{ZnCl}_2$  (Alfa Aesar, A16281) was utilized for density separation. Nile red dye (Tokyo Chemical Industry Co., N0659) was used for fluorescent tagging of MP. Additional staining using 4',6-diamidino-2-phenylindole or DAPI (Roche, 10236276001) was performed to check for the presence of biological material as described in S1c of Supplementary information (SI). Porcine pancreatic lipase (Merck, L3126) was used for in-situ lipase treatment (S1b of SI). Olympus SZX10 stereomicroscope (Olympus, Tokyo, Japan) equipped with SZX2-FGFPHQ filter set having excitation at 460–480 nm and emission at 495–540 nm was utilized for visualization of fluorescently stained MP. For chemical characterization, MP were placed in  $20 \mu\text{m}$  stainless steel filter mesh (KIAST, KF-STC2520) and analyzed using Bruker Lumos II  $\mu$ FTIR (Bruker, Bremen, Germany) imaging equipment.

### 2.2. Sample collection

Manila clams were purchased from the same vendor in Incheon complex fish market in May 2019. All clams were sourced from aquaculture farms in Mokpo, along the west coast of the Korean peninsula. Since there is a high possibility that the MP content may change during the transport of products from the place of production to the site of commerce (Cho et al., 2019), direct sampling of wild-caught or cultured samples was not conducted. For this reason, market samples of cultured clams were utilized to ensure that the quantity of MP closely matches with the amount that consumers are exposed to. In addition, washing of the soft tissue was avoided to take into account loosely bound MP that could also be eaten especially when food is consumed raw or steamed.

After purchase, clams were immediately stored in ice. Once in the laboratory, animals were wrapped in aluminum foil and stored at  $-20 \text{ }^\circ\text{C}$ . Shell length was measured using a caliper while samples are

frozen. The clams were segregated into two groups of significantly different size ( $p < 0.05$ ) based on shell length. The SC ( $n = 51$ ) had an average shell length of  $40.69 \pm 3.97$  mm, with a minimum of 31.79 mm and a maximum of 45.64 mm. In comparison, the LC ( $n = 50$ ) showed an average shell length of  $51.19 \pm 2.86$  mm, with a minimum of 46.18 mm and a maximum of 56.18 mm. The shell weight, soft tissue (wet) weight, and total weight of the two groups were also considerably different ( $p < 0.05$ ). Given these observations, the two groups of clams can be considered to be phenotypically distinct. A summary of the physical traits of SC and LC is displayed in Table 1. A detailed list containing the traits of all 101 Manila clams can be found in Table S1 (SI).

The age of the clams was also predicted based on their shell length using the von Bertalanffy growth curves of *Ruditapes philippinarum* reported in Korea (Choi et al., 2011). In this growth curve, the age of the clam (in years) is plotted in the x-axis and the corresponding shell length (in mm) in the y-axis. Through interpolation, SC are estimated to be approximately 2 1/2 years to 4 years of age, while LC are at least 5 years old.

Aside from the phenotypic distinctions, the clams were grouped in such a way to reflect the trend in wholesale market price of Manila clams. The average cost of SC is 13,375 Korean won for every 5 kg which is cheaper compared to 25,188 Korean won per 5 kg of LC (Noryangjin Fisheries Whoelsale, 2022). This price difference could influence the consumers choice and consumption due to economic reasons, which may pose an impact on the dietary exposure assessment.

### 2.3. Extraction of MP from clams

Frozen clam soft tissue was excised from the shell using a scalpel, weighed, and transferred to a glass digestion flask containing 250 mL of 10% (w/w) KOH solution at 60 °C. Thawing was avoided to prevent the loss of loosely attached MP, which could be carried away by the thawed liquid while removing the soft tissue from the shells or in case the tissue is sliced in the process. Only one clam was placed in each digestion flask. When the soft tissue wet weight of the clam exceeded 10 g, the sample was split into two similar pieces and digested separately. Sample digestion was conducted for 24 h at 60 °C while stirring (Dehaut et al., 2016). Prior to digestion, each solution was spiked with 10 pieces of green low-density polyethylene (LDPE) plastic bag cut into approximately 1 mm × 1 mm squares as a quality control measure (S2a of SI). After digestion, solutions were vacuum filtered using 47 mm GF/A filter paper, 1.6 μm pore size. The flasks were washed at least three times with 50 mL filtered deionized water to recover all spiked plastics. Blank solutions containing only filtered 10% KOH and LDPE spikes were always processed alongside samples to serve as negative controls.

### 2.4. Nile red staining of MP

The extracted MP were stained with NR following the procedure described in Maes et al. (2017). The GF/A filters containing MP were suspended in 10 mL ZnCl<sub>2</sub> aqueous solution ( $\rho = 1.37$  g/mL) and sonicated 3 times for 3 min. Obtained suspension was centrifuged and the upper layer was transferred into a glass test tube and stained by adding a filtered solution of 1 mg/mL NR in acetone at a final concentration of 10

**Table 1**

Summary of the phenotypic traits of small and large clams. Values are mean ± SD. Significant difference ( $p < 0.05$ ) between small and large clams is marked with an asterisk (\*).

Traits	Small clams (n = 51)	Large clams (n = 50)
Shell length (mm)*	40.69 ± 3.97	51.19 ± 2.86
Soft tissue wet weight (g)*	5.80 ± 1.16	11.21 ± 2.28
Shell weight (g)*	5.46 ± 0.10	9.12 ± 1.88
Total weight (g)*	11.26 ± 1.87	20.34 ± 3.77

μg/mL. Staining was performed for 30 min at 60 °C with constant shaking. The dyed MP were filtered using 25 mm GF/A filter (1.6 μm pore size) through vacuum filtration. Subsequently, the filter was washed with 50 mL absolute ethanol to remove excess dye and reduce background fluorescence.

### 2.5. Fluorescence microscopy and analysis of obtained images

Filter papers with NR-stained MP were viewed under Olympus stereomicroscope equipped with fluorescence filter (Ex 460–480 nm; Em 495–540 nm). For every section of the filter, fluorescent and bright-field images were both taken using DigiRetina 16 microscope camera. Images were captured at a resolution of 1600 × 1200 pixels and exposure time of 80 ms.

Slightly overlapping sectional photos were stitched together to create a high-quality composite image using Microsoft Image Composite Editor. Using ImageJ, color threshold was manually set and MP-ACT (Microplastics Automated Counting Tool) plug-in was applied to automatically count, measure, and classify the MP into fibers, fragments, and spherical particles based on their circularity (Prata et al., 2019). Circularity describes the resemblance of a particular shape to a circle, where a perfect circle is assigned the value of 1.0. MP with a circularity value of 0.0–0.3, 0.3–0.6, and 0.6–1.0 were classified as fibers, fragments, and (spherical) particles, respectively. The size of MP was based on feret diameter which is an approximation of the largest dimension of a fiber, fragment, or particle. The MP detected from the blanks ( $n = 15$ ) were also measured. The average MP quantity from the blank was subtracted from the corresponding categories of size and shape of MP from the samples to eliminate false positives. Additional information regarding the use of MP-ACT can be found in S2b of SI.

### 2.6. Chemical characterization by μFTIR imaging

Because of the interference caused by glass microfibers, NR-stained MP from GF/A filters were first transferred to 25 mm 20 μm stainless steel filter mesh. For this purpose, MP on several GF/A filters were transferred onto one stainless steel filter by re-suspending MP in ZnCl<sub>2</sub> through sonication followed by vacuum filtration. GF/A filters were chosen arbitrarily through random number selection to create a composite subsample. For the SC, 3 composite subsamples: S1 ( $n = 13$ ), S2 ( $n = 6$ ), and S3 ( $n = 11$ ), were made which contained a total of 30 clams. On the other hand, 5 composite subsamples: L1 ( $n = 4$ ), L2 ( $n = 8$ ), L3 ( $n = 6$ ), L4 ( $n = 8$ ), and L5 ( $n = 5$ ), were prepared for the LC comprising a total of 31 clams. This resulted to three and five steel filters, corresponding to the three and five composite subsamples of SC and LC, respectively. In the case of blanks, GF/A filters were treated individually.

Chemical characterization was performed using Lumos II μFTIR in the Korea Institute of Analytical Science and Technology (KIAST) using their in-house test method. The total filter area was scanned, and spectra were acquired from 600 to 4000 cm<sup>-1</sup> at 12 cm<sup>-1</sup> resolution. The FPA (focal plane array)-based imaging datasets were analyzed using siMPle (Systematic Identification of MicroPLastics in the Environment) (Conesa and Iniguez, 2020) which allowed automated size measurement and identification of the polymer types by matching sample spectra with the MPHunter reference library (Primpke et al., 2017; Liu et al., 2019). A minimum match of 60% and 40% in the range of 2700–3500 cm<sup>-1</sup> and 1000–1800 cm<sup>-1</sup>, respectively, was used as the criteria for polymer identification. At the same time, MP morphology was categorized into either fiber or non-fiber groups.

### 2.7. Characterization and classification of MP size and morphology

The feret diameter (largest distance between two points), which was automatically measured in ImageJ as described in Section 2.5, was used to estimate the size of MP. The size was divided into the following ranges

for classification: <50  $\mu\text{m}$ , 50–100  $\mu\text{m}$ , 100–150  $\mu\text{m}$ , 150–200  $\mu\text{m}$ , 200–250  $\mu\text{m}$ , 250–1000  $\mu\text{m}$ , 1000–2000  $\mu\text{m}$ , and > 2000  $\mu\text{m}$ . Note that the second number in the range was rounded to a whole number (e.g., 50–99.99  $\mu\text{m}$  to 50–100  $\mu\text{m}$ ) except for the range 1000–2000  $\mu\text{m}$ , where 2000  $\mu\text{m}$  refers to its true value. The <50  $\mu\text{m}$  group was changed to 20–50  $\mu\text{m}$  in the case of  $\mu\text{FTIR}$  due to the limitation of the technique in reliably detecting MP <20  $\mu\text{m}$ .

The predefined categories of morphology in MP-ACT (Prata et al., 2019), namely particles, fibers, and fragments, were used to classify MP according to shape after NRS (Section 2.5). On the other hand, the predefined categories in SIMPLe (fiber and non-fiber) (Conesa and Iniguez, 2020) was utilized in the case of  $\mu\text{FTIR}$  spectroscopy, as explained in Section 2.6.

## 2.8. Verification of methods used for MP profiling

Before the analysis of the collected clams, preliminary experiments in which the efficacy of the digestion method (Section 2.3), and suitability of staining method (Section 2.4) for MP from biological samples were performed. The procedures and results are discussed in detail in S1 (a) and S2 (a, b) of SI. For these experiments, eight in-house MP standards: polypropylene (PP), high-density polyethylene (HDPE), low-density polyethylene (LDPE), polyvinylchloride (PVC), polystyrene (PS), polyethylene terephthalate (PET), polycaprolactam (PA-6), and polyamide 66 (PA-66) were used. A total of nine consumer plastics (CP) were also used to verify the effectiveness of NRS on processed and weathered polymers (S1a of SI). The CPs include white Styrofoam (CP1), colorless water bottle (CP2), colorless microwaveable box (CP3), beige-colored microwaveable box (CP4), black plastic bag (CP5), resealable bag with blue print (CP6), food grade colorless resealable bag (CP7), white thread (CP8), and cream-colored yarn (CP9).

## 2.9. Dietary exposure assessment

The average intake of MP associated with the daily consumption of Manila clams in South Korea by Korean consumers was determined. For this purpose, consumption data (average of 1.25 g/person/day) from the latest Korean Consumption Survey were utilized (Ministry of Health and Welfare of Korea, 2015; Cho et al., 2019). Only the data obtained from  $\mu\text{FTIR}$  imaging were used for exposure assessment since overestimation in MP quantity was observed from NRS as discussed in detail in Section 3.5. For this analysis, L1 was excluded (Dixon's outlier test,  $p < 2.2\text{e}-16$ ).

The human exposure to MP via clams was estimated using three different exposure scenarios. The first one assumed the consumption of only SC while the second one assumed the consumption of only LC. The third exposure scenario did not differentiate between the size of clams. The general mean MP concentration was determined using the composite samples shown in Table S2. The estimation of dietary intake (EDI) per person was calculated as the number of MP consumed per person per day. The conservative annual consumption of MP was also determined, under the assumption that the clams were consumed daily, by multiplying daily intake by 365 days. Even though the average daily consumption value of 1.25 g/person/day does not incorporate a specific size group of clams, it was still used to estimate the EDI's for the first and second exposure scenarios to provide additional insights regarding factors that affect dietary exposure to MP. Having a separate calculation for the consumption of SC alone and LC alone is also important in view of the trend in market price as previously mentioned in Section 2.2.

In addition to the three exposure scenarios described above, the exposure at the level of each MP category (clam size  $\times$  MP range  $\times$  polymer type,  $n = 224$ ) was estimated. This was determined by multiplying each of the MP concentrations (per polymer type and size, and per clam size) expressed as MP/g clams by the daily consumption value of clams. Hereby, a simple assumption was made that only one MP category was present in a clam. In this way, the contribution of each MP

category to the total exposure was calculated.

To include uncertainties and variabilities of this approach, data were assigned the best fit distribution (weight of the individual clam samples and MP counts by  $\mu\text{FTIR}$  using Chi-square statistics). From all data points and their associated probability distributions, exposure based on Monte-Carlo simulation implemented in @Risk software (Palisade V8.0) was estimated. For this, randomly drawn MP concentrations (MP polymer/g) were multiplied by randomly drawn sample-based weight of individual clams. This was done 100,000 times, resulting in a distribution of 100,000 person-day dietary exposures for each identified MP category.

## 2.10. Data analysis

The unit MP/g was used to express the MP concentration relative to the wet weight of the soft tissue in grams, while MP/ind was used to express the number of MP per individual piece of clam. Normality of data was assessed using the Shapiro-Wilk method, homogeneity of variance using Levene's test, and subsequent mean comparison using Mann Whitney Wilcoxon test. A non-parametric evaluation was used because the obtained MP concentrations were not normally distributed, and variances were also not homogenous. However, the shell length and weight, soft tissue (wet) weight, and total weight of SC and LC passed the normality test but failed the test for homogeneity of variance. Because of this, Welch  $t$ -test was used to evaluate the difference between the means of the variables related to the physical traits of the clams.

The overestimation in NRS measurements were determined by first taking the difference between NRS and  $\mu\text{FTIR}$  results and calculating the ratio between this difference and the  $\mu\text{FTIR}$  value (expressed in percentage). The presence of associations between variables was tested through Spearman's correlation and the difference in the MP profiles between the groups was analyzed using principal component analysis (PCA). Statistical significance was determined at  $p < 0.05$ . All values are reported as mean  $\pm$  standard deviation and statistical analyses were conducted in RStudio version 1.3.959.

## 3. Results

### 3.1. Blank samples

A total of 15 blank measurements were conducted to check for contamination. An average of  $13 \pm 7$  MP was detected in blank samples through NRS. During the transfer of MP from the GF/A to the steel filter prior to  $\mu\text{FTIR}$  imaging, a minimal loss of MP was observed, i.e., a minimum of 1 to a maximum of 3 MP were lost from each filter. The blank measurement was subtracted from each sample to determine the final quantity of MP.

### 3.2. Profiling of MP in clams using Nile red staining

A total of 3692 MP were isolated from all samples ( $n = 101$ ), whereby 1078 originated from SC while 2614 were isolated from LC. The average MP concentration was  $4.25 \pm 5.21$  MP/g or  $36.55 \pm 58.34$  MP/ind for the combined clam size groups (Table 2). A broad range in MP content was observed in both groups, with SC exhibiting a span of 1–72 MP/ind and LC showing a span of 1–495 MP/ind. The SC and LC had a comparable concentration ( $p > 0.05$ ) of  $4.00 \pm 4.27$  and  $4.51 \pm 6.06$  MP/g, respectively. Conversely, LC contained significantly higher ( $p < 0.05$ ) MP numbers, when individual pieces of clam were considered:  $52.28 \pm 77.82$  MP/ind (LC) compared to  $21.14 \pm 19.56$  MP/ind in SC.

The semi-automated method for morphology measurement based on ImageJ resulted in three different morphology classifications: (spherical) particles, fragments, and fibers. In both SC and LC, particles were the most prominent shape category, accounting for 80–86 % of total MP. Fragments and fibers followed, with a prevalence of 10–13 % and 4–7 %, respectively.



**Table 2**

Profiles (quantity, shape, and size) of microplastics (MP/g and MP/individual) in small and large clams (SC and LC) based on Nile red staining (NRS) and  $\mu$ FTIR imaging.

Values are shown as a mean  $\pm$  standard deviation; The category non-fiber is only for  $\mu$ FTIR. This category covers both spherical particles and fragments; (\*) denotes significant difference at  $p < 0.05$  between SC and LC; Italicized values inside ( ) under NRS were obtained from composite samples of SC (n = 3, total of 30 clams) and LC (n = 5, total of 31 clams); <sup>a</sup>NRS data from SC (n = 51) and LC (n = 50); <sup>b</sup> $\mu$ FTIR data from composite samples of SC (n = 3, total of 30 clams) and LC (n = 5, total of 31 clams); <sup>c</sup>20–50  $\mu$ m; <sup>d</sup> $p = 0.057$ ; (NA) not applicable.

MP	Sample	MP/g		MP/individual	
		NRS <sup>a</sup>	$\mu$ FTIR <sup>b</sup>	NRS <sup>a</sup>	$\mu$ FTIR <sup>b</sup>
<b>Content</b>					
Total	All	4.25 $\pm$ 3.24 $\pm$	3.24 $\pm$ 1.56	36.55 $\pm$ 58.34	30.50 $\pm$ 19.09
		(3.82 $\pm$ 1.72)	(3.82 $\pm$ 1.72)	(34.39 $\pm$ 19.63)	(34.39 $\pm$ 19.63)
	SC	4.00 $\pm$ 4.27	2.70 $\pm$ 1.66	21.14 $\pm$ 19.56	15.64 $\pm$ 9.25
		(4.16 $\pm$ 2.01)	(4.16 $\pm$ 2.01)	(24.08 $\pm$ 11.08)	(24.08 $\pm$ 11.08)
	LC	4.51 $\pm$ 6.06	3.65 $\pm$ 1.59	52.28 $\pm$ 77.82*	41.63 $\pm$ 16.90
		(4.52 $\pm$ 1.58)	(4.52 $\pm$ 1.58)	(51.84 $\pm$ 16.35)	(51.84 $\pm$ 16.35)
<b>Shape</b>					
Spherical particles	SC	3.22 $\pm$ 3.70	NA	16.82 $\pm$ 17.01	NA
		0.26 $\pm$ 0.49	0.15 $\pm$ 0.23	1.53 $\pm$ 3.10	0.84 $\pm$ 1.30
Fibers	SC	0.52 $\pm$ 0.66	NA	2.78 $\pm$ 3.16	NA
		0.52 $\pm$ 0.66	NA	2.78 $\pm$ 3.16	NA
Fragments	SC	3.83 $\pm$ 5.83	NA	44.92 $\pm$ 75.07*	NA
		0.19 $\pm$ 0.37	0.57 $\pm$ 0.30	2.14 $\pm$ 4.07	6.49 $\pm$ 3.05 <sup>d</sup>
Spherical particles	LC	0.48 $\pm$ 0.77	NA	5.22 $\pm$ 8.12	NA
		0.48 $\pm$ 0.77	NA	5.22 $\pm$ 8.12	NA
Fibers	LC	NA	2.55 $\pm$ 1.44	NA	14.80 $\pm$ 8.03
		NA	2.55 $\pm$ 1.44	NA	14.80 $\pm$ 8.03
Fragments	LC	NA	3.07 $\pm$ 1.37	NA	35.15 $\pm$ 14.95
		NA	3.07 $\pm$ 1.37	NA	35.15 $\pm$ 14.95
<b>Size (<math>\mu</math>m)</b>					
<50	SC	1.34 $\pm$ 1.33	1.83 $\pm$ 0.80 <sup>c</sup>	7.63 $\pm$ 8.24	10.61 $\pm$ 4.45 <sup>c</sup>
		1.34 $\pm$ 1.33	1.83 $\pm$ 0.80 <sup>c</sup>	7.63 $\pm$ 8.24	10.61 $\pm$ 4.45 <sup>c</sup>
50–100	SC	1.80 $\pm$ 2.13	0.75 $\pm$ 0.71	9.43 $\pm$ 10.40	4.32 $\pm$ 3.99
		1.80 $\pm$ 2.13	0.75 $\pm$ 0.71	9.43 $\pm$ 10.40	4.32 $\pm$ 3.99
100–150	SC	0.40 $\pm$ 0.83	0.11 $\pm$ 0.16	1.92 $\pm$ 3.45	0.63 $\pm$ 0.89
		0.40 $\pm$ 0.83	0.11 $\pm$ 0.16	1.92 $\pm$ 3.45	0.63 $\pm$ 0.89
150–200	SC	0.16 $\pm$ 0.46	0.00 $\pm$ 0.00	0.71 $\pm$ 1.75	0.00 $\pm$ 0.00
		0.16 $\pm$ 0.46	0.00 $\pm$ 0.00	0.71 $\pm$ 1.75	0.00 $\pm$ 0.00
200–250	SC	0.07 $\pm$ 0.15	0.01 $\pm$ 0.01	0.39 $\pm$ 0.90	0.04 $\pm$ 0.08
		0.07 $\pm$ 0.15	0.01 $\pm$ 0.01	0.39 $\pm$ 0.90	0.04 $\pm$ 0.08
250–1000	SC	0.17 $\pm$ 0.35	0.01 $\pm$ 0.01	0.80 $\pm$ 1.56	0.04 $\pm$ 0.00
		0.17 $\pm$ 0.35	0.01 $\pm$ 0.01	0.80 $\pm$ 1.56	0.04 $\pm$ 0.00
1000–2000	SC	0.04 $\pm$ 0.11	0.00 $\pm$ 0.00	0.20 $\pm$ 0.49	0.00 $\pm$ 0.00
		0.04 $\pm$ 0.11	0.00 $\pm$ 0.00	0.20 $\pm$ 0.49	0.00 $\pm$ 0.00
>2000	SC	0.02 $\pm$ 0.07	0.00 $\pm$ 0.00	0.10 $\pm$ 0.36	0.00 $\pm$ 0.00
		0.02 $\pm$ 0.07	0.00 $\pm$ 0.00	0.10 $\pm$ 0.36	0.00 $\pm$ 0.00
<50	LC	1.31 $\pm$ 2.62*	2.74 $\pm$ 1.26 <sup>c</sup>	14.72 $\pm$ 28.18	31.21 $\pm$ 13.12 <sup>c</sup>
		1.31 $\pm$ 2.62*	2.74 $\pm$ 1.26 <sup>c</sup>	14.72 $\pm$ 28.18	31.21 $\pm$ 13.12 <sup>c</sup>
50–100	LC	2.05 $\pm$ 3.16	0.76 $\pm$ 0.29	24.32 $\pm$ 42.95*	8.65 $\pm$ 3.22
		2.05 $\pm$ 3.16	0.76 $\pm$ 0.29	24.32 $\pm$ 42.95*	8.65 $\pm$ 3.22
100–150	LC	0.60 $\pm$ 1.15*	0.11 $\pm$ 0.06	7.08 $\pm$ 15.69*	1.27 $\pm$ 0.67
		0.60 $\pm$ 1.15*	0.11 $\pm$ 0.06	7.08 $\pm$ 15.69*	1.27 $\pm$ 0.67
150–200	LC	0.20 $\pm$ 0.29*	0.02 $\pm$ 0.02	2.32 $\pm$ 3.82*	0.22 $\pm$ 0.31
		0.20 $\pm$ 0.29*	0.02 $\pm$ 0.02	2.32 $\pm$ 3.82*	0.22 $\pm$ 0.31
200–250	LC	0.13 $\pm$ 0.15*	0.02 $\pm$ 0.01	1.48 $\pm$ 1.67*	0.15 $\pm$ 0.10
		0.13 $\pm$ 0.15*	0.02 $\pm$ 0.01	1.48 $\pm$ 1.67*	0.15 $\pm$ 0.10
250–1000	LC	0.20 $\pm$ 0.35	0.02 $\pm$ 0.02	2.18 $\pm$ 3.54*	0.15 $\pm$ 0.20
		0.20 $\pm$ 0.35	0.02 $\pm$ 0.02	2.18 $\pm$ 3.54*	0.15 $\pm$ 0.20
1000–2000	LC	0.20 $\pm$ 0.35	0.02 $\pm$ 0.02	2.18 $\pm$ 3.54*	0.15 $\pm$ 0.20
		0.20 $\pm$ 0.35	0.02 $\pm$ 0.02	2.18 $\pm$ 3.54*	0.15 $\pm$ 0.20

**Table 2 (continued)**

MP	Sample	MP/g		MP/individual	
		NRS <sup>a</sup>	$\mu$ FTIR <sup>b</sup>	NRS <sup>a</sup>	$\mu$ FTIR <sup>b</sup>
>2000		0.02 $\pm$ 0.05	0.00 $\pm$ 0.00	0.18 $\pm$ 0.48	0.00 $\pm$ 0.00
		0.02 $\pm$ 0.05	0.00 $\pm$ 0.00	0.18 $\pm$ 0.48	0.00 $\pm$ 0.00
		0.00 $\pm$ 0.00	0.00 $\pm$ 0.00	0.02 $\pm$ 0.14	0.00 $\pm$ 0.00
		0.00 $\pm$ 0.00	0.00 $\pm$ 0.00	0.02 $\pm$ 0.14	0.00 $\pm$ 0.00

respectively. Relative to the weight of the samples, the concentration based on MP morphology was not significantly different ( $p > 0.05$ ). However, the individual pieces of LC had a substantially higher ( $p < 0.05$ ) concentration of particles at  $44.92 \pm 75.07$  particles/ind compared to  $16.8 \pm 17.0$  particles/ind obtained from the SC.

In terms of MP size, particles with feret diameters between 50 and 100  $\mu$ m were the most abundant in both clam groups and accounted for 44.6 % and 46.5 % of the total MP detected in the SC and LC groups, respectively. Plastic debris larger than 1 mm accounted for only 1.8 % of total MPs from both groups, making it the size with the lowest prevalence. LC had a higher concentration ( $p < 0.05$ ) of MP < 50, 100–150, 150–200, and 200–250  $\mu$ m at  $1.31 \pm 2.62$ ,  $0.60 \pm 1.15$ ,  $0.20 \pm 0.29$ , and  $0.13 \pm 0.15$  MP/g, respectively, compared to the  $1.34 \pm 1.33$ ,  $0.40 \pm 0.83$ ,  $0.16 \pm 0.46$ , and  $0.07 \pm 0.15$  MP/g observed from SC. Similarly, individual pieces of LC showed significantly higher levels ( $p < 0.05$ ) of MP at  $24.32 \pm 42.95$ ,  $7.02 \pm 15.69$ ,  $2.32 \pm 3.82$ ,  $1.48 \pm 1.67$ , and  $2.18 \pm 3.54$  MP/ind in the range of 50–100, 100–150, 150–200, 200–250, and 250–1000  $\mu$ m, respectively. In comparison, only  $9.43 \pm 10.40$ ,  $1.92 \pm 3.45$ ,  $0.71 \pm 1.75$ ,  $0.39 \pm 0.90$ ,  $0.80 \pm 1.56$  MP/ind was observed in SC belonging to the same size categories. The profiles of MP obtained in both groups of clams through NRS are displayed in Table 2, while Table S1 shows the MP profile in individual clams. As shown in Fig. 1A, correlation analysis only revealed moderate associations (Spearman's coefficient  $< 0.5$ ,  $p < 0.05$ ) between MP content and the phenotypic characteristics of the samples which include shell length and weight, (soft) tissue weight, and total weight. In addition, PCA analysis shows that SC and LC did not appear as distinct clusters in the PCA scores plot (Fig. 1C), and shell length only has a weak influence on the first two PC's (Fig. 1D).

### 3.3. Profiling of MP in clams using $\mu$ FTIR imaging

An average of  $3.24 \pm 1.56$  MP/g or  $30.50 \pm 19.09$  MP/ind were obtained when all sizes of clams were combined (Table 2). As a group, SC (S1 to S3) had  $2.70 \pm 1.66$  MP/g or  $15.64 \pm 9.25$  MP/ind, while LC (L1 to L5) showed  $3.65 \pm 1.59$  MP/g or  $41.63 \pm 16.90$  MP/ind according to  $\mu$ FTIR. The difference in MP content between the two groups was not significant ( $p > 0.05$ ). With regard to MP shape, the majority of MP were categorized as non-fibers which showed an average of  $2.55 \pm 1.44$  MP/g or  $14.80 \pm 8.03$  MP/ind, and  $3.07 \pm 1.37$  MP/g or  $35.15 \pm 14.95$  MP/ind for SC and LC, respectively. Table S2 (SI) shows the quantity of MP in each composite sample.

Due to analytical limitations, MP smaller than 20  $\mu$ m were excluded from the  $\mu$ FTIR analysis. The size range 20–50  $\mu$ m and 50–100  $\mu$ m were the two most prevalent in both groups of clams and contained particles which were primarily classified as non-fibers. The fibers, in contrast, exhibited a majority of feret diameters in the 50–100  $\mu$ m size range in SC and 20–50  $\mu$ m in LC. MP with feret diameters of 150–200  $\mu$ m and >1000  $\mu$ m were not observed in SC. Likewise, large particles >1000  $\mu$ m were not detected in LC. The concentrations of MP according to size and shape were all comparable ( $p > 0.05$ ) as shown in Table 2. In addition, only weak to moderate associations (Spearman's coefficient  $< 0.5$ ,  $p < 0.05$ ) were observed between MP concentration and shell length and weight, (soft) tissue weight, and total weight (Fig. 1B).

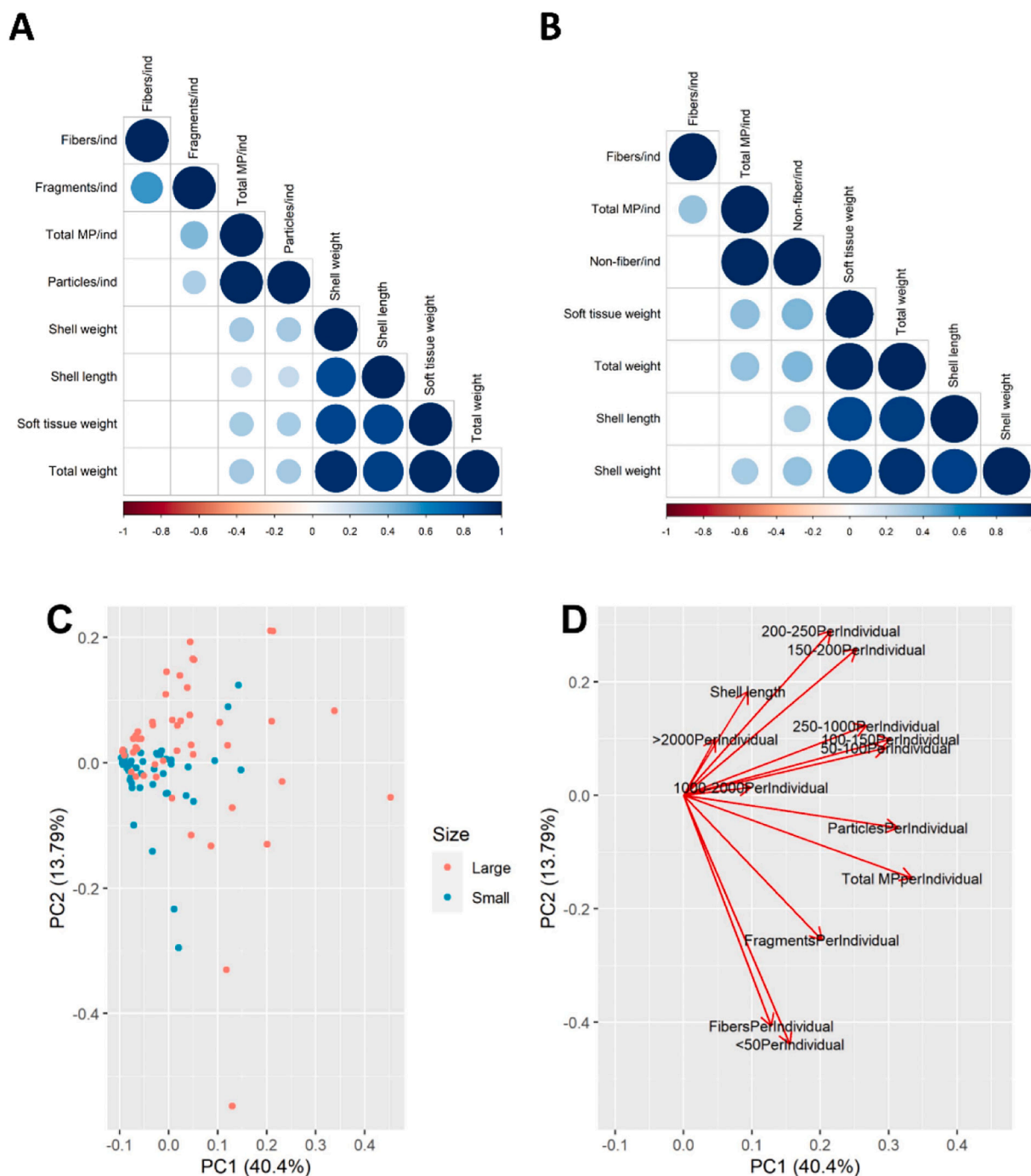


**Fig. 1.** Correlation matrix for the physical characteristics of clams (shell weight and length, soft tissue weight, and total weight) and microplastics concentration determined by (A) Nile Red staining and (B)  $\mu$ FTIR imaging. The size and color of the circles indicate the strength of correlation. Insignificant associations between variables are not shown. Principal component analysis of NRS-based measurements showing (C) scores plot for PC1 and PC2, and (D) loadings plot showing vectors of original variables. (For interpretation of the references to color in this figure legend, the reader is referred to the web version of this article.)

**3.4. Chemical characterization of MP in clams by  $\mu$ FTIR**

Four different synthetic polymers were identified from the isolated MP, namely, PE, PET, PP, and PS. Irrespective of the clam size, significantly higher ( $p < 0.05$ ) PET was present at  $0.66 \pm 0.68$  MP/g compared to PE with  $0.09 \pm 0.11$  MP/g. In addition, considerably more ( $p < 0.05$ ) PS ( $1.99 \pm 1.31$  MP/g) was detected than PE ( $0.09 \pm 0.11$  MP/g). Similar observations were obtained when concentration was expressed per individual clam. There was significantly higher ( $p < 0.05$ ) PET ( $5.14 \pm 4.36$  MP/ind) than PE ( $0.94 \pm 1.16$  MP/ind), PS ( $18.93 \pm 13.81$  MP/

ind) than PE ( $0.94 \pm 1.16$  MP/ind), and PS ( $18.93 \pm 13.81$  MP/ind) than PP ( $3.37 \pm 5.33$  MP/ind).

Between SC and LC, there were no notable differences ( $p > 0.05$ ) observed in the concentrations of each polymer in terms of both MP/ind and MP/g, as shown in Fig. 2A and B, respectively. However, PS was more prevalent ( $p < 0.05$ ) than PE and PET considering values from LC alone. On the other hand, no significant differences were observed between the polymers within SC.

Only PET and PS were detected in the fiber group in SC, while PP, PS, PE, and PET were all identified in the fibers isolated from LC, in

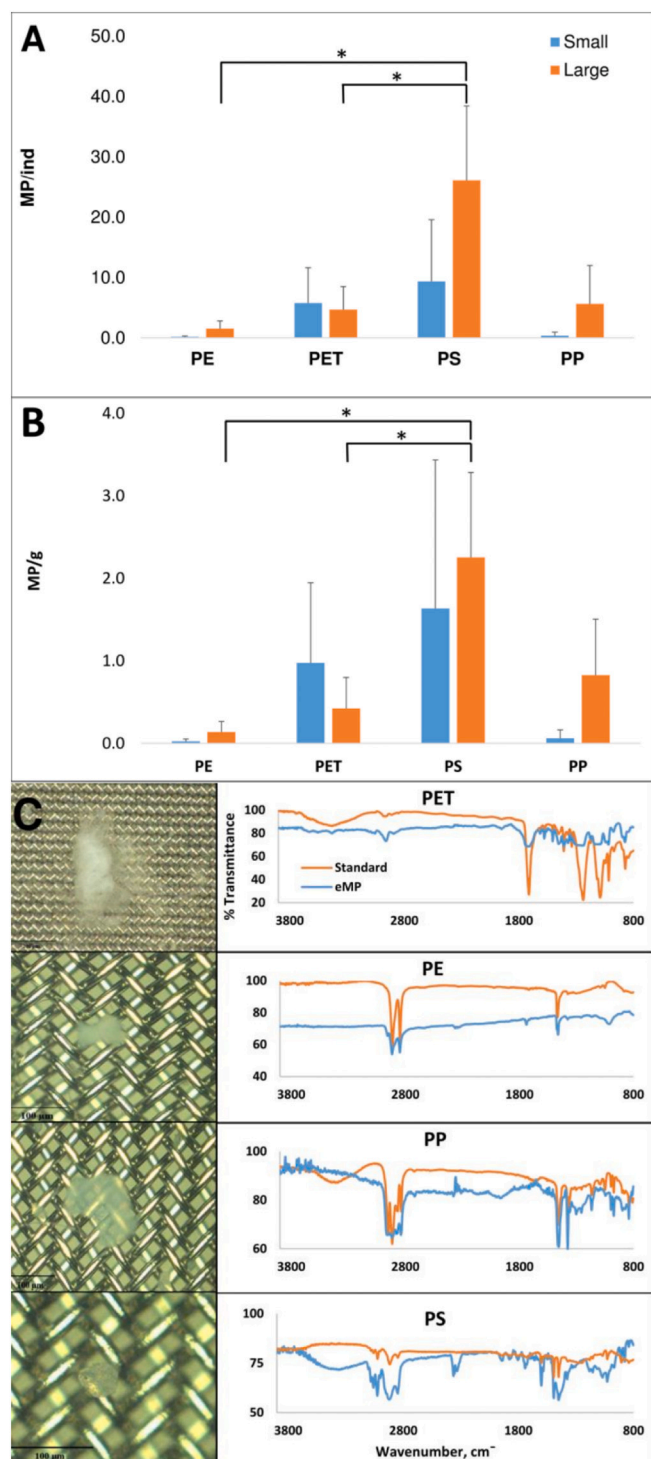


**Fig. 2.** Polymer concentrations in the small and large clams expressed as (A) MP/ind and (B) MP/g. (C) (left panel) Representative images of extracted microplastics (eMP) and (right panel) their corresponding FTIR spectra overlaid with spectra of the standards. Top to bottom: polyethylene terephthalate (PET), polyethylene (PE), polypropylene (PP), and polystyrene (PS). (\*) denotes significant difference between polymer types at  $p < 0.05$ .

descending order of quantity. All four polymers in SC were predominantly 20–50  $\mu\text{m}$ , corresponding to 72 % of the total quantity. Meanwhile, 25 % fell into the range 50–100  $\mu\text{m}$ . A similar trend was observed from LC. All polymers were primarily 20–50  $\mu\text{m}$  (74 %) and 50–100  $\mu\text{m}$  (21 %). Representative images of each polymer and their spectra are presented in Fig. 2C.

### 3.5. Comparison of results from NRS and $\mu\text{FTIR}$ imaging

The MP concentration was consistently lower when measured via  $\mu\text{FTIR}$ . Even when MP with diameters  $< 20 \mu\text{m}$  were subtracted from the NR-based measurement, the results from  $\mu\text{FTIR}$  were still lower. Taken altogether, the samples contained  $3.24 \pm 1.56 \text{ MP/g}$  ( $30.50 \pm 19.09 \text{ MP/ind}$ ) based on  $\mu\text{FTIR}$ , and  $3.82 \pm 1.72 \text{ MP/g}$  ( $34.39 \pm 19.63 \text{ MP/ind}$ ) based on NRS ( $p > 0.05$ ). The total MP from the composite samples of SC were 411 and 594 according to  $\mu\text{FTIR}$  and NRS, respectively. Within the LC group, only 1148 were detected through  $\mu\text{FTIR}$  compared to 1402 detected by NRS. In terms of concentration, there were  $4.16 \pm 2.01 \text{ MP/g}$  ( $24.08 \pm 11.08 \text{ MP/ind}$ ) and  $2.70 \pm 1.66$  ( $15.64 \pm 9.25 \text{ MP/ind}$ ) in SC according to NRS and  $\mu\text{FTIR}$ , respectively. In LC,  $4.52 \pm 1.58 \text{ MP/g}$  ( $51.84 \pm 16.35 \text{ MP/ind}$ ) were detected through NRS while  $3.65 \pm 1.59 \text{ MP/g}$  ( $41.63 \pm 16.90 \text{ MP/ind}$ ) were found using  $\mu\text{FTIR}$ . In summary, NRS analysis resulted in a 47.0 %, 23.7 %, and 75.0 % overestimation in SC (S1 to S3) and 686.2 %, 22.1 %, 45.5 %, 18.8 %, and 17.9 % overestimation in LC (L1 to L5), where 686.2 % was deemed an outlier (Dixon's test,  $p < 2.2e-16$ ) (Fig. 3). This translated to an average of  $48.6 \pm 25.7 \%$  increase in MP concentration in SC and a  $31.0 \pm 13.1 \%$  increase in concentration in LC.

The source of this overestimation was investigated by checking for remnants of biological material and lipid droplets coming from the clams. Co-staining of MP with DAPI (Stanton et al., 2019) revealed the presence of both NR- and DAPI-positive debris as shown in Fig. S8 of SI. The presence of these debris indicates traces of undigested organic matter from the clams still exists. To examine the presence of lipids, enzymatic treatment with lipase was performed (S1b of SI). However, even after 18 h of in-situ lipase treatment, the number of MP did not change (Fig. S10 of SI) which suggests that lipids were not the cause of overestimation. The remnants of undigested biological material from the clams most likely caused the overestimation in NRS. Despite the higher values from NRS, the concentrations (MP/g and MP/ind) obtained from the two methods were comparable ( $p > 0.05$ ).

The estimated size derived from NRS for the majority of MP was slightly larger at 50–100  $\mu\text{m}$ . In contrast,  $\mu\text{FTIR}$  measured predominantly MP with diameters between 20 and 50  $\mu\text{m}$ . MP in the range of 150–200  $\mu\text{m}$  were identified with NRS, but not  $\mu\text{FTIR}$  (Table 2). In terms of shape, the particle and fragment categories from NRS were combined to correspond to the non-fiber category from  $\mu\text{FTIR}$ . In this manner, both methods were parallel in detecting largely non-fibers.

### 3.6. Exposure assessment

Exposure was estimated assuming consumption of small and large clams separately, and all clams independent of their size. These three exposure scenarios based on the deterministic approach revealed a difference in exposure in relation to size of clams (Table 3).

EDI obtained for the scenario where clams were consumed independent of their size was 4.08 MP/person/day and 1489.37 MP/person/year. The latter is a conservative approach and may be further improved by obtaining a more detailed clams consumption frequency. Additionally, the contribution of each polymer to the total exposure assuming independent presence of each polymer was estimated. In this approach, MP polymer was expressed per clam resulting in 224 results. The best fitted distributions, clam weight input fitted by RiskBetaGeneral (0.16706, 0.16107, 5.6900, 12.2033), and MP per polymer fitted by RiskGamma (0.48512, 42.295), were used to estimate the exposure and subsequently calculate the contribution of each polymer to the total exposure.

Fig. 4 shows that PS contributes the most to the total exposure in both SC and LC. Interestingly, PET shows the second highest contribution in SC, while in LC, this is PP. Whereas for PET and PS which are both found in SC, there are various effect (toxicological) studies, PP appears to be understudied (de Ruijter et al., 2020). It is of note that in both SC and LC, the smallest particle diameters were the most abundant and

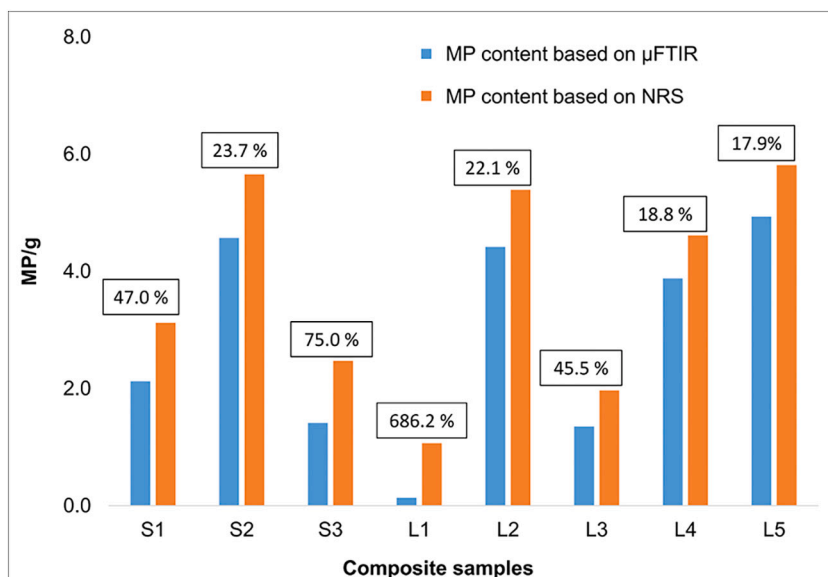


**Fig. 3.** Microplastics content based on  $\mu$ FTIR imaging and Nile Red staining (NRS) with indicated extent of overestimation (%) by NRS given in boxes. Note that L1 is an outlier (Dixon's test,  $p < 2.2e-16$ ). (For interpretation of the references to color in this figure legend, the reader is referred to the web version of this article.)

**Table 3**

Daily and annual estimated dietary intake (EDI) of MP via clams using three exposure scenarios.

	Scenarios		
	LC	SC	All clams
Concentration (MP/g)	3.65	2.70	3.24
Consumption of clams (g/person/day)	1.25	1.25	1.25
EDI –daily (MP/person/day)	4.56	3.38	4.08
EDI – annual (MP/person/year)	1663.17	1232.22	1489.37

might contribute the most to the exposure. Thus, the evaluation grouped according to various MP categories (size range and/or polymer type) may be useful for future risk characterization.

**4. Discussion**

The average MP concentration from both sizes of clams combined was  $4.25 \pm 5.21$  and  $3.24 \pm 1.56$  MP/g as measured through NRS and  $\mu$ FTIR, respectively. In comparison to other studies conducted in South Korea, 4–14 times higher MP abundance was observed considering only data from NRS. Similarly, 3–10 times more MP per gram of clam tissue was detected through  $\mu$ FTIR imaging. In 2019, Cho et al. only detected  $0.42 \pm 0.08$  MP/g in Manila clams from the west coast, while even less was seen on samples from the southern coast at  $0.29 \pm 0.13$  MP/g. A higher MP concentration was observed in samples from Cheonsu and Hampyeong (also in the western coast) at  $0.49 \pm 0.23$  and  $1.03 \pm 0.36$  MP/g, respectively (Cho et al., 2021). In this study, overestimation by NRS has been confirmed to be caused by the remaining biological matter from the samples which could explain the greater MP concentration relative to other studies. However,  $\mu$ FTIR data were solely obtained from

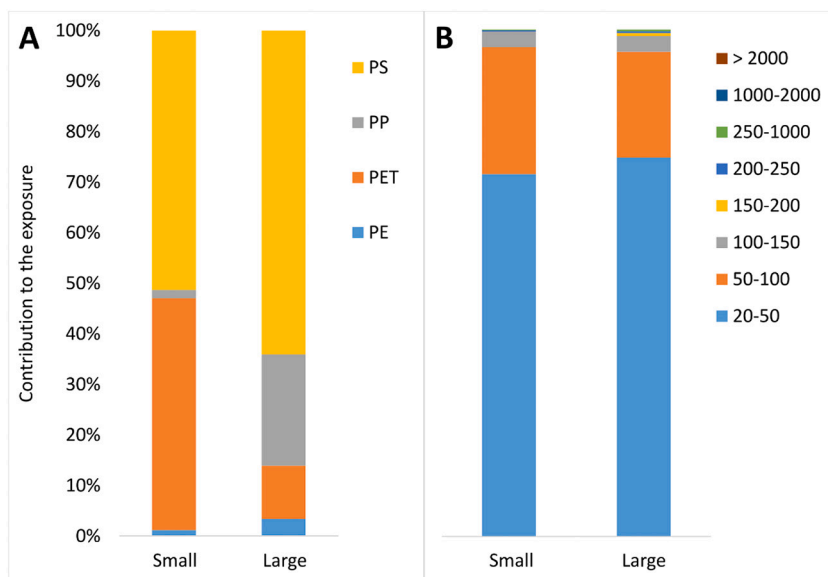


**Fig. 4.** Contribution to the total dietary exposure (%) of each MP category as a function of (A) polymer type and (B) size. PS- polystyrene, PP- polypropylene, PET- polyethylene terephthalate, and PE- polyethylene.



the isolated MP. In spite of this, the concentration was still higher than that of earlier investigations (Cho et al., 2019, 2021). This difference could be due to one or a combination of the following reasons: (1) sample preparation, (2) variation in environmental conditions and location of the source of samples, and (3) differences in analytical techniques used for MP isolation, organic matter digestion, and MP counting strategies.

First, loss of weakly-bound MP was prevented in this study by avoiding extensive washing of the sample and ensuring that the soft tissue was kept frozen while excising it from the shell. As a result, more MP were retained and quantified from the clams.

Second, the geographical source is a major contributing factor in MP ingestion by bivalves. The amount and characteristics of ingested MP is correlated with the level and status of plastic pollution in the animal's habitat (Beyer et al., 2017). The samples in this study were obtained from Mokpo's coastal zone which is characterized by extensive tidal flats and strong tides (Kang et al., 2009). An increase in semidiurnal (two low and two high tides per day) tidal amplitude was observed in this area as a consequence of dyke and sea wall constructions (Byun et al., 2004). As such, MP present in the water column are highly stirred, re-suspended, and pushed into the intertidal zone. This may have increased the encounter rate of the clams to MP leading to enhanced exposure. Setälä et al. (2016) observed that even at low concentration of PS beads, bivalves showed high uptake of particulates because of their filter-feeding strategy combined with the elevated encounter rate to PS (Setälä et al., 2016).

Lastly, the analytical approaches also have influence on the data. Compared to other studies which employed manual inspection and counting of MP (using  $\mu$ FTIR microscope), this study employed FPA-based  $\mu$ FTIR imaging which allowed scanning of the whole filter area to search for and identify MP. This prevented bias coming from user selection of spatially separated points on the filter which could lead to accidental omission of MP, especially transparent ones (Loder et al., 2015).

Aside from concentration, a discrepancy in shape was also observed between this study and earlier reports (Cho et al., 2019, 2021) where fragments were more abundant compared to (spherical) particles, which was the most prominent shape identified from both SC and LC (as determined by NRS). At first, this disagreement was thought to be due to lipid droplets from the clams, which was also considered as a possible source of overestimation in NRS as discussed in Section 3.5. The lipid droplets could have appeared as spherical fluorescent MP due to the affinity of NR to hydrophobic substances. However, as illustrated in Fig. S9 (SI), this was not the case. A lipid layer was present on the GF/A filter directly after NRS, but it completely disappeared after the ethanol washing step, leaving behind only fluorescent pieces of the spiked HDPE standard. Furthermore, we attempted enzymatic digestion (SI S1b) of the debris in-situ (directly on the filter) and the results are shown in Fig. S10 (SI). After lipase treatment, the quantity of MP did not change. This confirmed that the large quantity of particles detected in this study was not caused by lipids coming from the clams.

We have identified that the reason behind the mismatched results was the different strategies used for shape classification. In former studies, the shape was manually identified by the observer by following certain criteria (Cho et al., 2019, 2021; Jang et al., 2020). For instance, a fragment is irregularly shaped and appears to be chipped from a bigger piece of object while a (spherical) particle is round with a smooth surface. In this study, instead of visual descriptors, the shape was determined based on circularity determined through ImageJ.

In order to compare if the method based on circularity and manual observation of shape assign the same shape category, four images of MP considered as fragments were selected from previous investigation (Vinay Kumar et al., 2021). As shown in Fig. S11 (SI), the circularity of all fragments is 0.8 and above. Based on this value, our method identifies those MP as particles instead of fragments. This is another instance where different analytical approaches yield different results and

highlights the need for harmonization of analytical approaches used for MP characterization from environmental samples. The root cause of the problem is the lack of standardized methods in the field of MP research. Because of this, comparison of results found in numerous studies is challenging. There is a need to develop a standardized protocol for MP sampling, extraction, and detection for different types of samples. In addition, an international consensus on MP classification (morphology and size) should also be established (Li et al., 2019).

In this study, the clams were grouped according to size under the assumptions that the larger (and older) animals may bioaccumulate more MP and/or size of the animal has an effect on MP ingestion. The clams were carefully segregated to achieve two phenotypically distinct groups based on both shell length and soft tissue weight. Despite this substantial difference in size, correlation analysis (on data obtained from both NRS and  $\mu$ FTIR) did not show any strong and significant association between the MP content and physical characteristics of the samples. In addition, when PCA was applied to NRS data, SC and LC formed only one instead of two distinct groups as shown in Fig. 1 (C and D). This suggests that the MP profiles of SC and LC overlap with each other. The differently sized clams cannot be distinguished from one another just on the basis of their MP content. Similar observations were found in *Perna canaliculus* from New Zealand (Webb et al., 2019) and *Mytilus edulis* from the United Kingdom and Zealand (Scott et al., 2019).

As mentioned in Section 2.2, there was approximately at least 1-year age difference between LC and SC. In this case, LC may have been exposed longer to the MP present in its habitat leading to accumulation of more MP. This should have been evident in the measured mean value of MP/ind. MP/g is not an appropriate measure in this case because of the higher biomass of LC. According to NRS, LC contained substantially higher MP/ind compared to SC. On the contrary,  $\mu$ FTIR data indicated that the two groups have similar concentrations. Due to the proven overestimation in NRS, as discussed in detail in Section 3.5, only  $\mu$ FTIR-based measurements were considered. In this respect, LC did not accumulate more MP as initially postulated. This could be due to the natural process of waste excretion. Even when more MP were ingested through filter-feeding, more MP were also egested. Mussels were shown to quickly eliminate MP trapped in the gills as pseudo feces, while those that make their way into the gut are usually expelled as feces (Li et al., 2021). Li et al. (2016) proposed that the balance between feeding and egestion will allow MP accumulation to reach a steady state wherein the MP concentration remains at a stable range. However, the interplay between MP uptake and egestion is still not well understood at this time. The process is more complex especially since translocation and retention of MP in different parts of bivalves has been observed (Browne et al., 2008; Ward and Kach, 2009; Van Cauwenberghe et al., 2015). In addition, selective intake and elimination was also found to occur in oysters and mussels (Ward et al., 2019). More studies are needed to provide a better understanding of the dynamics of ingestion and egestion. Laboratory exposure studies involving longer exposure times will provide important insights into the behavior and fate of MP after ingestion by shellfish as it occurs in the natural environment.

The analogous concentration and type of synthetic polymers found in SC and LC suggest that there was a uniform distribution of the polymers in the animals' habitat. Previous studies involving Manila clams and other bivalves consistently reported the presence of PE, PET, PS, and PP (Li et al., 2015; Digka et al., 2018a; Phuong et al., 2018; Qu et al., 2018). PE and PET are widely used in the manufacture of plastic containers and food packaging such as water bottles, food wrappers, and bags (Teng et al., 2019). PS is commonly used in insulation materials, while PP is incorporated into clothing fibers, non-woven fabrics, filaments, and packaging films (Lithner et al., 2012; Teng et al., 2019). Aside from these sources, the materials used in shellfish aquaculture is also a contributor of MP. For instance, from the aquaculture, Pediveliger clam larvae are moved to the nursery where they are covered in mesh until they are mature enough for seeding (10–15 mm shell length) in intertidal sites. Nets made of PP or HDPE are also used to cover the clam beds as

protection against predation (Dumbauld et al., 2009).

In South Korea, several MP studies involving beach sediments and surface water frequently reported high quantities of PS, specifically ePS (expanded PS) (Heo et al., 2013; Kang et al., 2015; Lee et al., 2015). PS is cheap and is widely used in South Korea as packaging material and aquaculture buoys. An estimated 1.6 million ePS buoys are released per year which makes this material ubiquitous in Korean waters (MOF (Ministry of Oceans and Fisheries), 2017). PS was predominantly observed in both sizes of clams in this study, although its high concentration was not enough to be significant compared to the other polymers within SC. The samples may have been exposed to floating PS debris as the tide moved the suspended particles into the intertidal zone where clam farming usually takes place. Cho et al. (2019) reported that Manila clams grown in tidal flats contained more MP compared to bivalves cultured using deep water farming (i.e. mussels and oysters). This shows that current aquaculture practices and techniques could also contribute to the MP contamination of farmed bivalves. However, this may not be true in other regions. A previous study in British Columbia reported similar levels of MP contamination in farmed and wild Pacific oysters and Manila clams. Aside from this, plastic debris from the nets, ropes, or fences commonly used in shellfish culture did not match the MP identified from both species (Covernton et al., 2019). Based on this, it appears that the impact of aquaculture, and associated plastic equipment, on MP contamination in shellfish varies from case to case. Nevertheless, there is no indication to overlook its influence on the findings of this study.

Statistically, similar MP concentrations were obtained using NRS and  $\mu$ FTIR ( $p > 0.05$ ). However, it is important to acknowledge that NRS consistently generated higher MP quantities. For studies aiming at exposure assessment, NRS does not seem to be a suitable method since overestimated MP concentration will lead to unreliable estimates of human exposure. Given that overestimation was proven to be due to undigested organic matter, it seems that alkaline digestion in tandem with NRS is not a suitable method despite its repeated use in previous reports involving biota (Lv et al., 2019; Dowarah et al., 2020; Prata et al., 2021). In this respect, caution should be exercised by checking for remnants of biological material before the application of NRS. This could be achieved by co-staining approaches using DAPI or methylene blue that selectively binds nucleic acids (DNA or RNA), thereby revealing the presence of leftover biological matter (Stanton et al., 2019; Michelaraki et al., 2020).

The true nature of the organic remnants in this study is not clear and to identify them is beyond the scope of this investigation. Nevertheless, we have eliminated lipids as the source by performing lipase treatment, but it is possible that small fragments of tissues that may contain lipids which were not accessible to enzymatic treatment were present. The existence of protein-lipid complexes is also plausible. Unless organic matter is completely removed, the reliability of NRS-based MP measurement is uncertain. More efforts should be directed towards finding an effective digestion method for biological samples.

A number of assumptions were made for dietary exposure estimation because of the lack of detailed data on South Korean consumption of Manila clams. The available consumption data was only evaluated on a daily basis, so the average daily consumption was taken into account. In addition, a clear description is lacking with regards to the inclusion of shell weight in the average daily consumption value. Because of this, the consumption of 1.25 g/person/day was assumed to include only soft tissue weight. An additional limitation exists in terms of the representativeness of the sample since the Manila clams were obtained from only one market. This limitation affects the measured average concentration of MP that was used to derive the EDI's. Nevertheless, the EDI's still provide valuable insights regarding MP intake through clam consumption.

It is also important to note that both farmed and wild Manila clams are available in the Korean market. In 2019, a production of 23,773 tons and 22,254 tons of wild-caught and farmed Manila clams, respectively,

was recorded in South Korea. Approximately 35,250 tons of the total Manila clam production was consumed in the country on the same year (Ministry of Oceans and Fisheries in Republic of Korea, 2021). This study only focused on cultured Manila clams, but dietary exposure assessment and/or MP profiling could be improved in the future by taking both wild and farmed Manila clams to obtain a more representative sample. A number of studies already compared the MP content between cultured and wild bivalves, but results were not consistent. Some reported higher MP abundance in samples from the wild (Li et al., 2016; Cho et al., 2021) while others did not observe any differences (De Witte et al., 2014; Davidson and Dudas, 2016; Covernton et al., 2019). In any case, wild-caught samples should also be factored into the sampling strategy for future investigations.

Aside from the three exposure scenarios which highlight exposure to all MP of various sizes and polymer types, additional estimates were also generated to emphasize the impact of the four detected polymers. Even though only independent presence of each polymer was estimated, it could be beneficial in light of the influence of polymer composition to the fate of MP inside an organism (de Ruijter et al., 2020). Aside from particle size/diameter and polymer type, assessment based on surface area might also be worth considering for future risk characterization given that surface area was previously shown to be more predictive of adverse effects compared to particle size in PS particles (Brown et al., 2001).

## 5. Conclusion

This study provides a comprehensive comparison of the concentration, size, shape, and polymer type of MP present in market samples of farmed SC and LC by utilizing two of the most used techniques (NRS and  $\mu$ FTIR) in MP research. We have established that Manila clams from South Korea are highly contaminated with MP, but the size, weight, or age of the animal has no influence on the amount and characteristics of the MP detected. In addition, alkaline digestion was found to be insufficient which led to overestimation of MP content by NRS. In order to obtain more reliable results from NRS in the future, an efficient digestion method for biological samples has to be established. Until this is achieved, NRS-based quantification, especially in biota, should be used with caution and not taken independently. Taking into account that a long-term dietary exposure (annual) to MP is based on a daily consumption, and that the contribution of each MP category was based on the total weight of an individual clam, the approximated EDI probably overestimates the real exposure. On the other hand, only one marine species was taken into account and multiple reports suggests the presence of MP in various marine species used for human consumption. In order to assess the total dietary exposure to MP, an integrated approach capturing various food sources of MP is needed. In the case of bivalves, a detailed consumption data including only edible tissue weight is of utmost importance for better evaluation. Even though studies on toxicological dose–response relationships are still lacking, an extensive exposure assessment is a vital first step in establishing relevant health effects in the future.

Supplementary data to this article can be found online at <https://doi.org/10.1016/j.marpolbul.2022.113846>.

## CRedit authorship contribution statement

**Maria Krishna de Guzman:** Data curation, Formal analysis, Investigation, Methodology, Validation, Visualization, Writing – original draft, Writing – review & editing. **Mirjana Andjelković:** Formal analysis, Writing – original draft, Writing – review & editing. **Vesna Jovanović:** Formal analysis, Writing – review & editing. **Jaehak Jung:** Investigation, Writing – review & editing. **Juyang Kim:** Investigation. **Lea Ann Dailey:** Writing – review & editing. **Andreja Rajković:** Writing – review & editing. **Bruno De Meulenaer:** Writing – review & editing. **Tanja Ćirković Velicković:** Conceptualization, Funding

acquisition, Project administration, Resources, Supervision, Writing – review & editing.

### Declaration of competing interest

The authors declare that they have no known competing financial interests or personal relationships that could have appeared to influence the work reported in this paper.

### Data availability

Data will be made available on request.

### Acknowledgement

This study was supported by the Ghent University Global Campus; Special Research Fund (BOF) of Ghent University (grant number 01N01718); Serbian Academy of Sciences and Arts Project F-26; Horizon2020 project FoodEnTwin (grant number 810752); and IMPTOX European Union's Horizon 2020 research and innovation program (grant number 965173). We also thank Ho-min Park for services related to translating reports, websites, and other relevant documents from Korean to English.

### References

- Arthur, C., Baker, J.E., Bamford, H.A., 2009. Proceedings of the International Research Workshop on the Occurrence, Effects, and Fate of Microplastic Marine Debris. University of Washington Tacoma, Tacoma, WA, USA.
- Besseling, E., Wegner, A., Foekema, E.M., Van Den Heuvel-Greve, M.J., Koelmans, A.A., 2013. Effects of microplastic on fitness and PCB bioaccumulation by the lugworm *Arenicola marina* (L.). *Environ. Sci. Technol.* 47, 593–600.
- Beyer, J., Green, N.W., Brooks, S., Allan, I.J., Ruus, A., Gomes, T., Bråte, I.L.N., Schøyen, M., 2017. Blue mussels (*Mytilus edulis* spp.) as sentinel organisms in coastal pollution monitoring: a review. *Mar. Environ. Res.* 130, 338–365. <https://doi.org/10.1016/j.marenvres.2017.07.024>.
- Brown, D.M., Wilson, M.R., MacNee, W., Stone, V., Donaldson, K., 2001. Size-dependent proinflammatory effects of ultrafine polystyrene particles: a role for surface area and oxidative stress in the enhanced activity of ultrafines. *Toxicol. Appl. Pharmacol.* 175, 191–199.
- Browne, M.A., Dissanayake, A., Galloway, T.S., Lowe, D.M., Thompson, R.C., Galloway, T.S., Thompson, R.C., 2008. Ingested microscopic plastic translocates to the circulatory system of the mussel, *Mytilus edulis* (L.) ingested microscopic plastic translocates to the circulatory system of the mussel, *Mytilus edulis* (L.). *Environ. Sci. Technol.* 42, 5026–5031. <https://doi.org/10.1021/es800249a>.
- Browne, M.A., Crump, P., Niven, S.J., Teuten, E., Tonkin, A., Galloway, T., Thompson, R., 2011. Accumulation of microplastic on shorelines worldwide: sources and sinks. *Environ. Sci. Technol.* 45, 9175–9179. <https://doi.org/10.1021/es201811s>.
- Byun, D.S., Wang, X.H., Holloway, P.E., 2004. Tidal characteristic adjustment due to dyke and seawall construction in the mokpo coastal zone. *Korea. Estuar. Coast. Shelf Sci.* 59, 185–196. <https://doi.org/10.1016/j.eccs.2003.08.007>.
- Cabernard, L., Roscher, L., Lorenz, C., Gerdt, G., Primpke, S., 2018. Comparison of raman and fourier transform infrared spectroscopy for the quantification of microplastics in the aquatic environment. *Environ. Sci. Technol.* 52, 13279–13288. <https://doi.org/10.1021/acs.est.8b03438>.
- Cadée, G.C., 2002. Seabirds and floating plastic debris. *Mar. Pollut. Bull.* 44, 1294–1295.
- Canesi, L., Ciacci, C., Bergami, E., Monopoli, M.P., Dawson, K.A., Papa, S., Canonico, B., Corsi, I., 2015. Evidence for immunomodulation and apoptotic processes induced by cationic polystyrene nanoparticles in the hemocytes of the marine bivalve *mytilus*. *Mar. Environ. Res.* 111, 34–40.
- Cho, Y., Joon, W., Jang, M., Myung, G., Hee, S., Shim, W.J., Jang, M., Han, G.M., Hong, S.H., 2019. Abundance and characteristics of microplastics in market bivalves from South Korea. *Environ. Pollut.* 245, 1107–1116. <https://doi.org/10.1016/j.envpol.2018.11.091>.
- Cho, Y., Shim, W.J., Jang, M., Han, G.M., Hong, S.H., 2021. Nationwide monitoring of microplastics in bivalves from the coastal environment of Korea. *Environ. Pollut.* 270, 116175. <https://doi.org/10.1016/j.envpol.2020.11.015>.
- Choi, Y.-M., Yoon, S.-C., Lee, S.-I., Kim, J.-B., Yang, J.-H., Yoon, B.-S., Park, J.-H., 2011. The study of stock assessment and management implications of the Manila clam, *Ruditapes philippinarum* in Taehwa river of Ulsan. *Korean J. Malacol.* 27, 107–114. <https://doi.org/10.9710/kjm.2011.27.2.107>.
- Cole, M., Lindeque, P., Halsband, C., Galloway, T.S., 2011. Microplastics as contaminants in the marine environment: a review. *Mar. Pollut. Bull.* 62, 2588–2597. <https://doi.org/10.1016/j.marpolbul.2011.09.025>.
- <collab>Ministry of Health and Welfare of Korea, K.C.for D.C.and P.</collab>, 2015. The Sixth Korea National Health and Nutrition Examination Survey (KNHANES VI). Conesa, J.A., Iniguez, M.E., 2020. Analysis of microplastics in food samples. In: *Handbook of Microplastics in the Environment*. Springer, pp. 1–16.
- Covernton, G.A., Collicutt, B., Gurney-Smith, H.J., Pearce, C.M., Dower, J.F., Ross, P.S., Dudas, S.E., 2019. Microplastics in bivalves and their habitat in relation to shellfish aquaculture proximity in coastal British Columbia, Canada. *Aquac. Environ. Interact.* 11, 357–374. <https://doi.org/10.3354/aei00316>.
- Cox, K.D., Covernton, G.A., Davies, H.L., Dower, J.F., Juanes, F., Dudas, S.E., 2019. Human consumption of microplastics. *Environ. Sci. Technol.* 53, 7068–7074.
- Davidson, K., Dudas, S.E., 2016. Microplastic ingestion by wild and cultured Manila clams (*Venerupis philippinarum*) from Baynes Sound, British Columbia. *Arch. Environ. Contam. Toxicol.* 71, 147–156. <https://doi.org/10.1007/s00244-016-0286-4>.
- de Ruijter, V.N., Redondo-Hasselerharm, P.E., Gouin, T., Koelmans, A.A., 2020. Quality criteria for microplastic effect studies in the context of risk assessment: a critical review. *Environ. Sci. Technol.* 54, 11692–11705.
- De Witte, B., Devriese, L., Bekaert, K., Hoffman, S., Vandermeersch, G., Cooreman, K., Robbens, J., 2014. Quality assessment of the blue mussel (*Mytilus edulis*): comparison between commercial and wild types. *Mar. Pollut. Bull.* 85, 146–155. <https://doi.org/10.1016/j.marpolbul.2014.06.006>.
- Dehaut, A., Cassone, A.L., Frère, L., Hermabessiere, L., Himber, C., Rinnert, E., Rivière, G., Lambert, C., Soudant, P., Huvet, A., Duflos, G., Paul-Pont, I., 2016. Microplastics in seafood: benchmark protocol for their extraction and characterization. *Environ. Pollut.* 215, 223–233. <https://doi.org/10.1016/j.envpol.2016.05.018>.
- Deng, Y., Zhang, Y., Lemos, B., Ren, H., 2017. Tissue accumulation of microplastics in mice and biomarker responses suggest widespread health risks of exposure. *Sci. Rep.* 7, 1–10. <https://doi.org/10.1038/srep46687>.
- Digka, N., Tsangaris, C., Kaberi, H., Adamopoulou, A., Zeri, C., 2018a. Microplastic abundance and polymer types in a Mediterranean environment. In: Proceedings of the International Conference on Microplastic Pollution in the Mediterranean Sea. Springer, pp. 17–24. <https://doi.org/10.1007/978-3-319-71279-6>.
- Digka, N., Tsangaris, C., Torre, M., Anastasopoulou, A., Zeri, C., 2018b. Microplastics in mussels and fish from the northern Ionian Sea. *Mar. Pollut. Bull.* 135, 30–40. <https://doi.org/10.1016/j.marpolbul.2018.06.063>.
- Dowarah, K., Patchaiyappan, A., Thirunavukkarasu, C., Jayakumar, S., Devipriya, S.P., 2020. Quantification of microplastics using Nile red in two bivalve species *Perna viridis* and *Meretrix meretrix* from three estuaries in Pondicherry, India and microplastic uptake by local communities through bivalve diet. *Mar. Pollut. Bull.* 153, 110982. <https://doi.org/10.1016/j.marpolbul.2020.110982>.
- Dris, R., Gasperi, J., Mandin, C., Tassin, B., 2016. A First Overview of Textile Fibers, Including Microplastics, in Indoor and Outdoor Environments A First Overview of Textile Fibers, Including Microplastics, in Indoor and. <https://doi.org/10.1016/j.envpol.2016.12.013>.
- Dumbauld, B.R., Ruesink, J.L., Rumrill, S.S., 2009. The ecological role of bivalve shellfish aquaculture in the estuarine environment: a review with application to oyster and clam culture in west coast (USA) estuaries. *Aquaculture* 290, 196–223.
- Elert, A.M., Becker, R., Duemichen, E., Eisentraut, P., Falkenhagen, J., Sturm, H., Braun, U., 2017. Comparison of different methods for MP detection: what can we learn from them, and why asking the right question before measurements matters? *Environ. Pollut.* 231, 1256–1264. <https://doi.org/10.1016/j.envpol.2017.08.074>.
- Eriksen, M., Lebreton, L.C.M.M., Carson, H.S., Thiel, M., Moore, C.J., Borror, J.C., Galgani, F., Ryan, P.G., Reisser, J., 2014. Plastic pollution in the world's oceans: more than 5 trillion plastic pieces weighing over 250,000 tons afloat at sea. *PLoS One* 9, e111913. <https://doi.org/10.1371/journal.pone.0111913>.
- Food and Agriculture Organization of the United Nations (FAO), 2016. FAOSTAT. Food and Agriculture Organization Food Balance Sheet [WWW Document].
- González-Soto, N., Hatfield, J., Katsumiti, A., Drouidier, N., Lacave, J.M., Bilbao, E., Orbea, A., Navarro, E., Cajaraville, M.P., 2019. Impacts of dietary exposure to different sized polystyrene microplastics alone and with sorbed benzo [a] pyrene on biomarkers and whole organism responses in mussels *Mytilus galloprovincialis*. *Sci. Total Environ.* 684, 548–566.
- Green, D.S., 2016. Effects of microplastics on european flat oysters, *Ostrea edulis* and their associated benthic communities. *Environ. Pollut.* 216, 95–103.
- Heo, N.W., Hong, S.H., Han, G.M., Hong, S., Lee, J., Song, Y.K., Jang, M., Shim, W.J., 2013. Distribution of small plastic debris in cross-section and high strandline on Heungnam beach, South Korea. *Ocean Sci. J.* 48, 225–233. <https://doi.org/10.1007/s12601-013-0019-9>.
- Jang, M., Shim, W.J., Cho, Y., Han, G.M., Song, Y.K., Hong, S.H., 2020. A close relationship between microplastic contamination and coastal area use pattern. *Water Res.* 171, 115400. <https://doi.org/10.1016/j.watres.2019.115400>.
- Kang, J.W., Moon, S.-R., Park, S.-J., Lee, K.-H., 2009. Analyzing Sea level rise and tide characteristics change driven by coastal construction at mokpo coastal zone in Korea. *Ocean Eng.* 36, 415–425.
- Kang, J.H., Kwon, O.Y., Lee, K.W., Song, Y.K., Shim, W.J., 2015. Marine neustonic microplastics around the southeastern coast of Korea. *Mar. Pollut. Bull.* 96, 304–312. <https://doi.org/10.1016/j.marpolbul.2015.04.054>.
- Khoironi, A., Anggoro, S., Sudarno, 2018. The existence of microplastic in Asian green mussels. In: *IOP Conference Series: Earth and Environmental Science* 131. IOP Publishing, p. 012050.
- Lee, J., Lee, J.S., Jang, Y.C., Hong, S.Y., Shim, W.J., Song, Y.K., Hong, S.H., Jang, M., Han, G.M., Kang, D., Hong, S., 2015. Distribution and size relationships of plastic marine debris on beaches in South Korea. *Arch. Environ. Contam. Toxicol.* 69, 288–298. <https://doi.org/10.1007/s00244-015-0208-x>.
- Li, J., Yang, D., Li, L., Jabeen, K., Shi, H., 2015. Microplastics in commercial bivalves from China. *Environ. Pollut.* 207, 190–195. <https://doi.org/10.1016/j.envpol.2015.09.018>.



- Li, J., Qu, X., Su, L., Zhang, W., Yang, D., Kolandhasamy, P., Li, D., Shi, H., 2016. Microplastics in mussels along the coastal waters of China. *Environ. Pollut.* 214, 177–184. <https://doi.org/10.1016/j.envpol.2016.04.012>.
- Li, J., Liu, H., Chen, J.P., 2018. Microplastics in freshwater systems: a review on occurrence, environmental effects, and methods for microplastics detection. *Water Res.* 137, 362–374.
- Li, J., Lusher, A.L., Rotchell, J.M., Deudero, S., Turra, A., Bråte, I.L.N., Sun, C., Shahadat Hossain, M., Li, Q., Kolandhasamy, P., Shi, H., 2019. Using mussel as a global bioindicator of coastal microplastic pollution. *Environ. Pollut.* 244, 522–533. <https://doi.org/10.1016/j.envpol.2018.10.032>.
- Li, J., Wang, Z., Rotchell, J.M., Shen, X., Li, Q., Zhu, J., 2021. Where are we? Towards an understanding of the selective accumulation of microplastics in mussels. *Environ. Pollut.* 286, 117543. <https://doi.org/10.1016/j.envpol.2021.117543>.
- Lithner, D., Nordensvan, I., Dave, G., 2012. Comparative acute toxicity of leachates from plastic products made of polypropylene, polyethylene, PVC, acrylonitrile-butadiene-styrene, and epoxy to *Daphnia magna*. *Environ. Sci. Pollut. Res.* 19, 1763–1772.
- Liu, F., Olesen, K.B., Borregaard, A.R., Vollertsen, J., 2019. Microplastics in urban and highway stormwater retention ponds. *Sci. Total Environ.* 671, 992–1000.
- Loder, M., Gunner, G., Löder, M.G.J., Gerdt, G., 2015. Methodology Used for the Detection and Identification of Microplastics—A Critical Appraisal, *Marine Anthropogenic Litter*. Springer International Publishing, Cham. [https://doi.org/10.1007/978-3-319-16510-3\\_8](https://doi.org/10.1007/978-3-319-16510-3_8).
- Lu, Y., Zhang, Y., Deng, Y., Jiang, W., Zhao, Y., Geng, J., Ding, L., Ren, H., 2016. Uptake and accumulation of polystyrene microplastics in zebrafish (*Danio rerio*) and toxic effects in liver. *Environ. Sci. Technol.* 50, 4054–4060.
- Lv, L., Qu, J., Yu, Z., Chen, D., Zhou, C., Hong, P., Sun, S., Li, C., 2019. A simple method for detecting and quantifying microplastics utilizing fluorescent dyes - safranin T, fluorescein isophosphate, Nile red based on thermal expansion and contraction property. *Environ. Pollut.* 255, 113283 <https://doi.org/10.1016/j.envpol.2019.113283>.
- Maes, T., Jessop, R., Wellner, N., Haupt, K., Mayes, A.G., 2017. A rapid-screening approach to detect and quantify microplastics based on fluorescent tagging with Nile red. *Sci. Rep.* 7, 44501.
- Mallory, M.L., 2008. Marine plastic debris in northern fulmars from the Canadian high Arctic. *Mar. Pollut. Bull.* 56, 1501–1504.
- Mathalon, A., Hill, P., 2014. Microplastic fibers in the intertidal ecosystem surrounding Halifax Harbor, Nova Scotia. *Mar. Pollut. Bull.* 81, 69–79. <https://doi.org/10.1016/j.marpolbul.2014.02.018>.
- Michelarakaki, M., Joseph, O., Karnik, S., Devalla, S., Madanan, K., Prabhu, R., 2020. Potential for Nile red dye-based analysis of microplastics from oceanic samples. In: 2020 Glob. Ocean. 2020 Singapore - U.S. Gulf Coast, pp. 6–9. <https://doi.org/10.1109/IEEECONF38699.2020.9389207>.
- Ministry of Oceans and Fisheries in Republic of Korea, 2021. Survey on the Status of the Seafood Production and Distribution Industry in 2020.
- MOF (Ministry of Oceans and Fisheries), 2017. Establishment of Integrated Management System for Waste Aquaculture Styrofoam Buoy (in Korean).
- Mohsen, M., Sun, L., Lin, C., Huo, D., Yang, H., 2021. Mechanism underlying the toxicity of the microplastic fibre transfer in the sea cucumber *Apostichopus japonicus*. *J. Hazard. Mater.* 416, 125858 <https://doi.org/10.1016/j.jhazmat.2021.125858>.
- Ng, K.L., Obbard, J.P., 2006. Prevalence of microplastics in Singapore's coastal marine environment. *Mar. Pollut. Bull.* 52, 761–767.
- Noryangjin Fisheries Wholesale, 2022. Bidding price by fish type [WWW Document]. <https://www.susansijang.co.kr/nsis/miw/ko/info/miw3130>.
- Phuong, N.N., Poirier, L., Pham, Q.T., Lagarde, F., Zalouk-Vergnoux, A., 2018. Factors influencing the microplastic contamination of bivalves from the french Atlantic coast: location, season and/or mode of life? *Mar. Pollut. Bull.* 129, 664–674. <https://doi.org/10.1016/j.marpolbul.2017.10.054>.
- Plee, T.A., Pomory, C.M., 2020. Microplastics in sandy environments in the Florida keys and the panhandle of Florida, and the ingestion by sea cucumbers (Echinodermata: Holothuroidea) and sand dollars (Echinodermata: Echinoidea). *Mar. Pollut. Bull.* 158, 111437 <https://doi.org/10.1016/j.marpolbul.2020.111437>.
- Prata, J.C., Reis, V., Matos, J.T.V., da Costa, J.P., Duarte, A.C., Rocha-Santos, T., 2019. A new approach for routine quantification of microplastics using Nile red and automated software (MP-VAT). *Sci. Total Environ.* 690, 1277–1283.
- Prata, J.C., Alves, J.R., da Costa, J.P., Duarte, A.C., Rocha-Santos, T., 2020. Major factors influencing the quantification of Nile red stained microplastics and improved automatic quantification (MP-VAT 2.0). *Sci. Total Environ.* 719, 137498.
- Prata, J.C., Sequeira, I.F., Monteiro, S.S., Silva, A.L.P., da Costa, J.P., Dias-Pereira, P., Fernandes, A.J.S., da Costa, F.M., Duarte, A.C., Rocha-Santos, T., 2021. Preparation of biological samples for microplastic identification by Nile red. *Sci. Total Environ.* 783, 147065 <https://doi.org/10.1016/j.scitotenv.2021.147065>.
- Primpke, S., Lorenz, C., Rascher-Friesenhausen, R., Gerdt, G., 2017. An automated approach for microplastics analysis using focal plane array (FPA) FTIR microscopy and image analysis. *Anal. Methods* 9, 1499–1511.
- Qu, X., Su, L., Li, H., Liang, M., Shi, H., 2018. Assessing the relationship between the abundance and properties of microplastics in water and in mussels. *Sci. Total Environ.* 621, 679–686. <https://doi.org/10.1016/j.scitotenv.2017.11.284>.
- Rainieri, S., Barranco, A., 2019. Microplastics, a food safety issue? *Trends food sci Technol.* 84, 55–57.
- Renzi, M., Guerranti, C., Bla, A., 2018. In: *Microplastic Contents From Maricultured and Natural Mussels*, 131, pp. 248–251. <https://doi.org/10.1016/j.marpolbul.2018.04.035>.
- Rist, S.E., Assidqi, K., Zamani, N.P., Appel, D., Perschke, M., Huhn, M., Lenz, M., 2016. Suspended micro-sized PVC particles impair the performance and decrease survival in the asian green mussel *Perna viridis*. *Mar. Pollut. Bull.* 111, 213–220. <https://doi.org/10.1016/j.marpolbul.2016.07.006>.
- Scott, N., Porter, A., Santillo, D., Simpson, H., Lloyd-Williams, S., Lewis, C., 2019. Particle characteristics of microplastics contaminating the mussel *Mytilus edulis* and their surrounding environments. *Mar. Pollut. Bull.* 146, 125–133. <https://doi.org/10.1016/j.marpolbul.2019.05.041>.
- Setälä, O., Norkko, J., Lehtiniemi, M., 2016. Feeding type affects microplastic ingestion in a coastal invertebrate community. *Mar. Pollut. Bull.* 102, 95–101.
- Shruti, V.C., Pérez-Guevara, F., Roy, P.D., Kutralam-Muniasamy, G., 2022. Analyzing microplastics with Nile red: emerging trends, challenges, and prospects. *J. Hazard. Mater.* 423 <https://doi.org/10.1016/j.jhazmat.2021.127171>.
- Stanton, T., Johnson, M., Nathanail, P., Gomes, R.L., Needham, T., Burson, A., 2019. Exploring the efficacy of Nile red in microplastic quantification: a costaining approach. *Environ. Sci. Technol. Lett.* 6, 606–611. <https://doi.org/10.1021/acs.estlett.9b00499>.
- Sussarellu, R., Suquet, M., Thomas, Y., Lambert, C., Fabioux, C., Pernet, M.E.J., Le Goïc, N., Quillien, V., Mingant, C., Epelboin, Y., Corporeau, C., Guyomarch, J., Robbens, J., Paul-Pont, I., Soudant, P., Huvet, A., 2016. Oyster reproduction is affected by exposure to polystyrene microplastics. *Proc. Natl. Acad. Sci. U. S. A.* 113, 2430–2435. <https://doi.org/10.1073/pnas.1519019113>.
- Teng, J., Wang, Q., Ran, W., Wu, D., Liu, Y., Sun, S., Liu, H., Cao, R., Zhao, J., 2019. Microplastic in cultured oysters from different coastal areas of China. *Sci. Total Environ.* 653, 1282–1292.
- Thompson, R.C., Olsen, Y., Mitchell, R.P., Davis, A., Rowland, S.J., John, A.W.G.G., McGonigle, D., Russell, A.E., Olson, Y., Mitchell, R.P., Davis, A., Rowland, S.J., John, A.W.G.G., McGonigle, D., Russell, A.E., 2004. Lost at sea: where is all the plastic? *Science* 80-.). 304, 838. <https://doi.org/10.1126/science.1094559>.
- Van Cauwenbergh, L., Janssen, C.R., 2014. Microplastics in bivalves cultured for human consumption. *Environ. Pollut.* 193, 65–70. <https://doi.org/10.1016/j.envpol.2014.06.010>.
- Van Cauwenbergh, L., Vanreusel, A., Mees, J., Janssen, C.R., 2013. Microplastic pollution in deep-sea sediments. *Environ. Pollut.* 182, 495–499. <https://doi.org/10.1016/j.envpol.2013.08.013>.
- Van Cauwenbergh, L., Claessens, M., Vandegheuchte, M.B., Janssen, C.R., 2015. Microplastics are taken up by mussels (*Mytilus edulis*) and lugworms (*Arenicola marina*) living in natural habitats. *Environ. Pollut.* 199, 10–17. <https://doi.org/10.1016/j.envpol.2015.01.008>.
- Vandermeersch, G., Van Cauwenbergh, L., Janssen, C.R., Marques, A., Granby, K., Fait, G., Kotterman, M.J.J., Diogène, J., Bekaert, K., Robbens, J., Devriese, L., 2015. A critical view on microplastic quantification in aquatic organisms. *Environ. Res.* 143, 46–55. <https://doi.org/10.1016/j.envres.2015.07.016>.
- Vinay Kumar, B.N., Lösche, L.A., Imhof, H.K., Löder, M.G.J., Laforsch, C., 2021. Analysis of microplastics of a broad size range in commercially important mussels by combining FTIR and raman spectroscopy approaches. *Environ. Pollut.* 269, 116147 <https://doi.org/10.1016/j.envpol.2020.116147>.
- Von Moos, N., Burkhardt-Holm, P., Köhler, A., 2012. Uptake and effects of microplastics on cells and tissue of the blue mussel *Mytilus edulis* L. after an experimental exposure. *Environ. Sci. Technol.* 46, 11327–11335. <https://doi.org/10.1021/es302332w>.
- Ward, J.E., Kach, D.J., 2009. Marine aggregates facilitate ingestion of nanoparticles by suspension-feeding bivalves. *Mar. Environ. Res.* 68, 137–142.
- Ward, J.E., Zhao, S., Holohan, B.A., Mladinich, K.M., Griffin, T.W., Wozniak, J., Shumway, S.E., 2019. Selective ingestion and egestion of plastic particles by the blue mussel (*Mytilus edulis*) and eastern oyster (*Crassostrea virginica*): implications for using bivalves as bioindicators of microplastic pollution. *Environ. Sci. Technol.* 53, 8776–8784. <https://doi.org/10.1021/acs.est.9b02073>.
- Webb, S., Ruffell, H., Marsden, I., Pantos, O., Gaw, S., 2019. Microplastics in the New Zealand green lipped mussel *Perna canaliculus*. *Mar. Pollut. Bull.* 149 <https://doi.org/10.1016/j.marpolbul.2019.110641>.
- Yang, D., Shi, H., Li, L., Li, J., Jabeen, K., Kolandhasamy, P., 2015. Microplastic pollution in table salts from China. *Environ. Sci. Technol.* 49, 13622–13627.